Accelerating Searches for Binary Pulsars

Jintao Luo and Scott M. Ransom[1]
National Radio Astronomy Observatory, Charlottesville, VA 22903
jluo@nrao.edu

ABSTRACT

With this paper we present our work on accelerating searches for binary pulsars using graphics processing units (GPUs). The detectability of pulsars in binary systems is reduced by Doppler smearing due to the orbital motion. Techniques called as "acceleration" searches have been developed to mitigate this loss in sensitivity. We speed up the Fourier-domain acceleration search utilizing Nvidia GPUs. As the best performance, the GPU-powered acceleration search achieves up to ∼80 times speedup factor over the single-core CPU version.

Subject headings: pulsar search: acceleration search: GPU: CUDA

1. Introduction

Pulsars are recognized as rotating neutron stars. Binary pulsars, those in binary systems, are of particular interest for studying relativistic physics, see, for example **?**. Since the initial discovery of pulsars(**?**) , numerous surveys have been carried out to enlarge the number of known pulsars, especially binary pulsars. Searching for new pulsars is a difficult task, although it is conceptually simple, since it requires intensive computations. For isolated pulsars, the search procedure includes searching the dispersion measure(DM) and the spin period of the pulsar. When search for a binary pulsar, there are additional difficulties introduced by the orbital motion. Due to the Doppler shift, the period changes during the observation and the sensitivity of the search is much reduced.

Several techniques have been developed to alleviate this kind of orbital motion-caused sensitivity loss(e.g. **?**). These so called "acceleration" searches operate on either the time domain or the frequency domain. However, extensive computing power is required for implementing these techniques. Generally the largest part of working time is spent on the process of acceleration search when searching for a binary pulsar.

Benefiting from Nvidia's CUDA language, we speed up the frequency-domain acceleration search technique developed by Scott Ransom. This acceleration is achieved by porting the program from C to CUDA C. The implementation with standard off-the-shelf GPUs produces a speedup factor of ∼80 times, as the best result, over the single-core CPU version.

2. Acceleration Search

2.1. Orbital Acceleration

The pulsed signal from a solitary pulsar with a rotation period P_p can be represented as a sum of Fourier components:

$$S_p(t) = \sum_{k=1}^{\infty} a_k \exp(ik\omega_p t + i\psi_k), \tag{1}$$

where $\omega_p = 2\pi/P_p$ is the angular frequency of the pulsar, and $a_k \exp(i\psi_k)$ is the complex amplitude of the kth harmonic. Then this signal's Fourier power spectrum, noted as $P(\omega)$, is:

$$P(\omega) = |\mathcal{F}[S_p(t)]|^2 = |\int_0^T S_p(t)\exp(-i\omega t)dt|^2; \tag{2}$$

Here T is the length of the observation.

For binary pulsars, the changing velocity, as a result of the orbital motion, leads to a changing

[1] Astronomy department, University of Virginia.

pulse period. Assume the pulsar's distance to the observer $d(t)$ is changing with time t. The pulsar signal emitted at time t would reach the observer at time $t + d(t)/c$. Here we can write the received signal $S_R(t)$ as:

$$S_R(t) = \sum_{k=1}^{\infty} a_k \exp\{ik\omega_p[t + d(t)/c] + i\psi_k\}. \quad (3)$$

Expanding $d(t)$ in a Taylor series:

$$d(t) = d(0) + v(0)t + a(0)\frac{t^2}{2!} + j(0)\frac{t^3}{3!} + \ldots. \quad (4)$$

Here $v(t)$, $a(t)$ and $j(t)$ represent the instantaneous velocity, acceleration, and rate of change of acceleration respectively. Then equation (3) can be rewritten as:

$$S_R(t) = \sum_{k=1}^{\infty} a_k \exp[\frac{ik\omega_p d(0)}{c}] \exp[ik\omega_p t(1 + \frac{v(0)}{c})] \times exp[\frac{ik\omega_p a(0)t^2}{2!c}] \exp[\frac{ik\omega_p j(0)t^3}{3!c}] \ldots. \quad (5)$$

According to this equation, the distance factor $d(0)$ only contributes by introducing a phase shift $\omega_p d(0)$. The velocity factor, $v(0)$, results in displacing harmonics from $k\omega_p$ to $k\omega_p(1+v(0)/c)$. This effect of displacement is not measurable since the period of a pulsar is unknown during a search. The contribution of higher order factors is to degrade the amplitude of the harmonics in the power spectrum.

When searching for binary pulsars, the signal to noise is decreased by the significant contribution from the acceleration factor a(0). To increase the sensitivity of the search, the acceleration-caused loss must be mitigated.

2.2. Acceleration Search Techniques

? made a brief review on techniques commonly used in searching for binary pulsars. A variety of so called "acceleration" searches have been developed to increase the sensitivity in searching for binary pulsars. When $T_{obs} \lesssim P_{orb}/10$, the drift of the pulsar rotating frequency caused by orbital motion is approximately linear hence it allows these acceleration searches to mitigate the loss in sensitivity almost completely. Using the recent acceleration search techniques, binary systems with orbital periods as short as ~ 90 minutes have been discovered(**?**).

The direct idea to perform the acceleration search is to resample the time series, stretching or compressing the data to compensate for a constant frequency derivative, and then apply Fourier transform on the resulting series. This time-domain strategy is adopted by traditional acceleration searches. Another idea is to implement the search in Fourier-domain. This method computes Fourier response over portions of the frequency-frequency derivative ($f - \dot{f}$) plane by correlating a predicted Fourier response with a subset of the complex Fourier amplitudes in the initial full-length FFT. In this method only local Fourier amplitudes from an FFT of the whole dataset are used.

Compared to their time-domain counterparts, Fourier-domain acceleration searches have several significant advantages:

1. Fourier methods do not change the statistics of the data because they do not require stretching or compressing the time series while time domain methods usually do them using linear interpolation.

2. The Fourier techniques use fewer FFTs as for each de-dispersed data only one single-length FFT is required. As the contrast, the time-domain techniques need to perform FFT for each trial acceleration.

3. Correlations used in the Fourier-domain search can be performed in core memory since only localized Fourier amplitudes are used. The fact the calculation is based on short FFTs and pre-computed templates allows efficient parallelization of Fourier-domain searches.

4. $f - \dot{f}$ trials could be calculated independently.

3. Algorithm of Fourier-domain Acceleration Search

In this section we describe the algorithm of the Fourier-domain acceleration search technique developed by **?**.

Consider a signal with a normalized Fourier response of A_{k-r_o}, where $k - r_o$ is simply the frequency offset of bin k from some reference frequency r_o, which goes to zero as $|k-r_o|$ approaches some number of bins $m/2$. The complex-valued Fourier response of such a signal at frequency r_o can be calculated with the sum

$$A_{r_o} \simeq \sum_{k=[r_o]-m/2}^{[r_o]+m/2} A_k A^*_{r_o-k} \tag{6}$$

If r_o is initially unknown we simply compute this summation at a range of frequencies r. Calculating this equation over a range of evenly spaced frequencies is equivalent of correlating the raw FFT amplitude with the template and is therefore most efficiently computed using short FFTs and the convolution theorem.

In the procedure of data process of practical pulsar searches, the raw data recorded in an observation first gets de-dispersed with a set of DM trials. The next step is to transform resulting time series into frequency domain using FFTs. To "sweep-up" the frequency range of interest, FFTs of length M, which is usually set to values of $1024, 2048, \ldots, 8192$ in practical use, together with the overlap-and-save or overlap-and-add techniques are used to implement correlations.

Consider a time series $D(n)$ produced by dedispersing the raw data with a certain DM, the Fourier-domain acceleration search procedure consists of following steps:

1. Transform $D(n)$ into Fourier-domian with a FFT. Here we get $F(r)$.
2. Select a range of the FFT result $F(r)$: F_{r1} $-$ F_{r2}, where $r1$ and $r2$ are determined by the frequency range of interest. To correlate these selected frequency amplitudes via FFT-based correlations, expand them with a padding method to form a new series $F^{'}$.
3. Correlate $F^{'}$ with a pre-computed template to generate a $f - \dot{f}$ plane.
4. Search for candidates from the resulting $f - \dot{f}$ plane.

4. CUDA implementation for Fourier-domain Acceleration Search

Using the Nvidia CUDA C language, we have implemented the Fourier-domain acceleration search on GPUs[1]. As shown in figure **??**, the implementation computationally comprises these parts:

1. Transform the data, which is the padded Fourier bins, to generate $F^{'}$ using a $M-$ *point* FFT.
2. Transform the correlation kernels using FFTs.
3. Time $F^{'}$ with one template plane, which is a $N{\times}M$ array where N is the number of accelerations trials.
4. IFFT the resulting $N{\times}M$ array and calculate its power.
5. Do harmonic summing if necessary.
6. Run candidates search using a specific threshold.

The FFT/IFFT, complex-valued multiplication, power calculation, harmonic summing and candidate searching have been moved onto the GPU, while the reset work like candidate optimization are left on the CPU. These computations involve one $M-$point FFT, $N{\times}M$ complex-valued multiplications and $N{\times}M$ IFFTs. If harmonic summing is needed to be done, array mapping and summing will occur and the number of additions will be determined by the number of harmonics to be summed. Candidate searching at the last step is relatively less computational.

4.1. FFT and IFFT

The time complexity of a $M-$point FFT/IFFT is $\mathcal{O}(M \times \log M)$. If N IFFTs are calculated one by one, the time complexity then is $\mathcal{O}(N \times M \times \log M)$. The simplest way to parallelize multiple FFTs with CUDA is using Nvidia's CuFFT library in batch mode. In practical uses, M is between 1024 and 8192, and N could be as large as a few thousands. Assuming M is 8192 and N

[1] Our code is available at: https://github.com/jintaoluo/presto

is 5000, there will be 5000 FFTs with length of 8192 to be calculated. The data volume then is $5000 \times 8192 \times 4$ = 156 MByte. This can be easily fit to modern GPUs, which are usually equipped with more than 2 GByte on-chip memories.

In concept, it is required to Fourier transform the templates to implement FFT-based correlations. Since the resulting planes are reusable, they can be stored as constant coefficients after being pre-calculated. Then significant computing resources get saved by avoiding calculating these planes repeatedly.

4.2. Complex-valued Multiplication

$F^{'}$ times the template plane's N rows and multiplications are done point-to-point. These complex-valued multiplications are independent from each other, then can be carried out in parallel on GPUs. The use of GPU's texture memory helps enhance the performance. If the template plane's size is relatively small, it can be bound to the texture memory together with $F^{'}$ to improve the read access to their contents.

4.3. Power Calculation

Powers of results from the correlation are calculated for the following candidate searching operation. A part of a FFT-based correlation's output need to be discarded or "chopped" because they are not valid products. So computing power then can be saved by only carrying out power calculations on the valid correlation output.

Like complex-valued multiplications, power calculations are applied to each single data point individually. That means it could benefit from the GPU's intrinsic parallelization capability as well.

4.4. Harmonic Summing

Duty cycles of pulsar signals generally range between 1% and 50%(**?**), resulting between 1 and 50 harmonics in their power spectrums. Taking advantage of this fact, "harmonic summing" of the power spectrum of the de-dispersed time series is utilized to increase the sensitivity in searches.

To do harmonic summing, conceptually, the power in the Fourier transform at frequencies $2f$, $3f$, $\ldots$, nf are summed with the one at frequency $1f$. Taking $\dot{f}$ into consideration, harmonic summing then becomes to add a harmonic's $f - \dot{f}$ plane to the fundamental plane. The amount of harmonics to sum up is determined by the input parameter *numharm*. Generally, he harmonic plane's size is smaller and needs to be scaled to the size of the fundamental one. In our implementation, the scale-up is realized by using a mapping method. To save computing resources, mapping indexes are pre-calculated with CPU and then stored on GPU. Additions are computed in parallel since each point in the fundamental plane gets added with only one point from the hramonic plane.

2D texture memory is used to improve data accesses to scale-up indexes and harmonic planes. Access to GPU's global memory, in which the on-GPU data is stored by default, is relatively time consuming. To minimize the number of this kind of access, harmonic summing is carried out together with the power calculation. If a point in the harmonic plane is usable, which means it will be used for power calculation and then harmonic summing, it will be read out only once. The following computations, power calculation and adding, will be placed in the same thread to save time.

4.5. Candidate Searching

The candidate searching follows harmonic summing to check the summed powers with a threshold. The qualified candidates, whose values are larger than the threshold, will be stored in the GPU's global memory and transfered back to the CPU later. The stored content includes not only the data value, but also other information like the corresponding frequency. This operation benefits from the use of texture memory as well. Like aforementioned power calculation, comparisons in candidate searching are done on each point independently. So they can be carried out in parallel. However counting the total number of qualified candidates should be done carefully, since it is likely multiple qualified candidates would request to modify the counter simultaneously. This risk is avoided via using a lock strategy realized with the use of atomic CUDA addition.

5. Results

The Fourier-domain acceleration search technique developed by Scott Ransom was realized as a program within PRESTO(PulsaR Exploration and Search TOolkit) which is a large suite of pulsar search and analysis software. Instead of creating a new individual program, our GPU-powered acceleration search code was developed as a patch or expansion to the original CPU-only program.

To test the code, files containing pulsed signals was generated using fake pulsar generator within PRESTO. Additionally, data recorded in real observations were used as well. Details of the three machines used to carry out these tests are listed in table **??**. And we have some cooperators help test the code with their own data and machines.

5.1. Fake data

Table **??** lists parameters which were used to generate fake data files. These files were generated as time series with different amounts of data points.

Figure **??** shows the performance on machine #1 when processing fake files. A Nvidia GTX 780 GPU was used to run the CUDA implementation code. And one of the 12 cores in a 3.20 GHz Intel Xeon E5-1650 CPU was used to do the CPU implementation. For both implementations, as shown in igure **??**, the general tendency is for total runtime to increase linearly as the number of data points increases. The parameter *zmax* was set to 256, and values of *numharm* are given in the figure's description.

Benchmarks on machines previously introduced are used to produce plots in figure **??**. On each machine, the GPU did the acceleration search on a group of fake files, with *zmax* set to 256 and *numharm* assigned as 1 and 16. The CPU's performance is used to calculate speedup factors.

As figure **??** shows, most benchmarks using 1 harmonics produce larger speedup factors than their 16-harmonic counterparts. Among results from machine #2 there are two exceptions. And there is one exception in results from machine #3. The smaller *numharm* means fewer harmonic summing operations. When this parameter is set to 1, there is completely no harmonic summing to be done. The fact that smaller *numharm* produces better speedup factor suggests that optimizing the on-GPU harmonic summing could lead to further improvement to our CUDA implementation.

5.2. Real data

Data from an observation on Terzan5 using GBT was used as real data to test the GPU-powered acceleration search code. The observation was made on Jul. 5, 2012, with a total bandwidth of 800 MHz centering round the frequency of 1105 MHz. A DM value of 239.93 was used to de-disperse the search mode raw data. The dedispersion produced files with various lengths of data points. The sampling time in resulting files is 40.96 μs.

Tests were carried out with machine #1. The parameter *numharm* was set to 8, and *zmax* was assigned values 5, 20, 50, 200, and 500. As shown in figure **??**, larger *zmax* results in higher speedup. And similar to curves in figure **??**.(a), which represents results on machine #1 processing fake data, speedup factors increase as the number of data points increases. However in figure **??** the curve for 500-*zmax* does not strictly follow this tendency, having less data point produces better speedup factor. This might be due to the noise level fluctuations in the raw data, which results in different noise levels in dedispersed files with different lengths.

6. Conclusions and Discussions

We have implemented a Fourier-domain acceleration search technique on GPUs using CUDA. This has led to a GPU-over-CPU performance speedup, which varies depending on parameter configurations and GPUs and CPUs that are used, of up to 80x.

Conclusions can be made from benchmarks on simulation and real data files:

1. Generally the larger data length produces larger GPU-on-CPU speedup factor.

2. Larger *zmax* would cause higher speedup factor.

3. Smaller *numharm* responds to larger speedup factor.

The explanation to *zmax*'s effect is there are more FFTs to be done when *zmax* is larger. And GPUs work pretty well in accelerating FFT computations. So the more FFTs, the larger speedup factor.

The reason why smaller *numharm*, not the larger one, produces the higher speedup factor is the on-GPU implementation for harmonic summing is not as good as for FFTs which utilize Nvdia's cuFFT library.

Work is ongoing with plans to maximize the usage of GPUs by using multithread technique. It is expected the current performance can be doubled.

7. Acknowledgments

This work is supported by the NSF PIRE award.

REFERENCES

Eatough, R. H. 2009, PhD thesis, University of Manchester

Hewish, A., Bell, S. J., Pilkington, J. D. H., Scott, P. F., & Collins, R. A. 1968,Nature, 217, 709

Johnston, H. M., & Kulkarni, S. M. 1991, AJ, 368, 504

Kulkarni, S. R., & Anderson, S. B. 1996, in IAU Symp. 174, Dynamical Evolution of Star Clusters: Confrontation of Theory and Observations, ed. P. Hut & J. Makino (Dordrecht: Kluwer), 181

Lyne, A. G. 1995, in ASP Conf. Ser. 72, Millisecond Pulsars: A Decade of Surprise, ed. A. S. Fruchter, M. Tavani, & D. C. Backer (San Francisco: ASP), 35

Middleditch, J., & Kristian, J. 1984, ApJ, 279, 157

Ransom, S. M., Eikenberry, S. S., & Middleditch, J. 2002, AJ, 124, 1788

Ransom, S. M., Cordes, J. M., & Eikenberry, S. S. 2003, ApJ, 589, 911

Taylot, J.H., Weisberg, J.M. 1989, ApJ, 345, 434

Table 1: Platforms Used in Investigations.

Machine	GPU	CPU	System Memory
1	Nvidia Geforce GTX 780	Intel Xeon E5-1650	62 GByte
2	Nvidia Geforce GTX 780	Intel Xeon E5-2640	63 GByte
3	Nvidia Geforce GTX Titan	Intel Xeon E5-2670	126 GByte

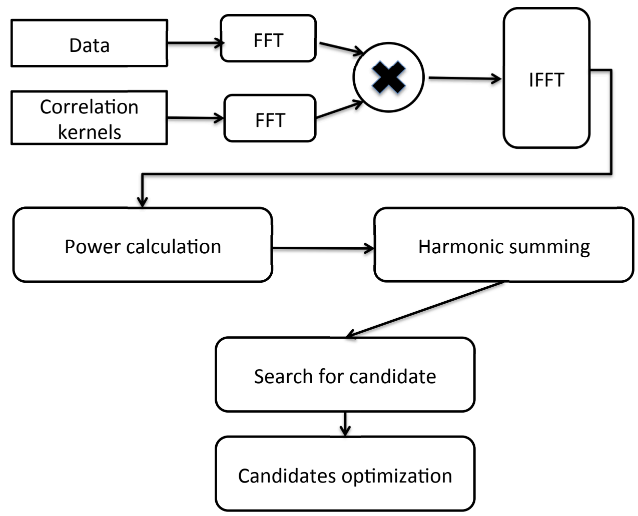

Fig. 1.— The block diagram of Fourier-domain acceleration search.

Table 2: Parameters used to generate fake file.

Parameter	Value
Sample time	64 μs
Pulse Frequency(f)	123.876876786 Hz
$\dot{f}$	1.123e-6 s^{-2}
Noise Sigma	14.142135623731

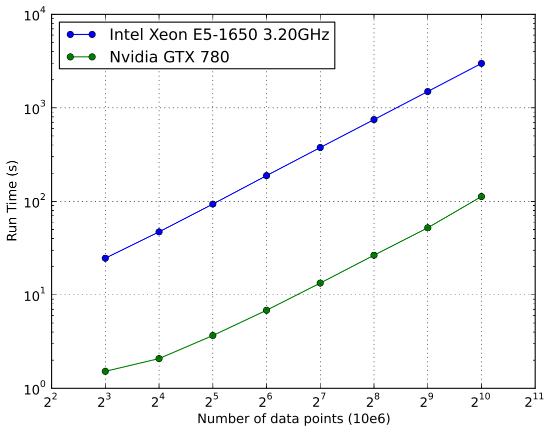

(a) 1 harmonic

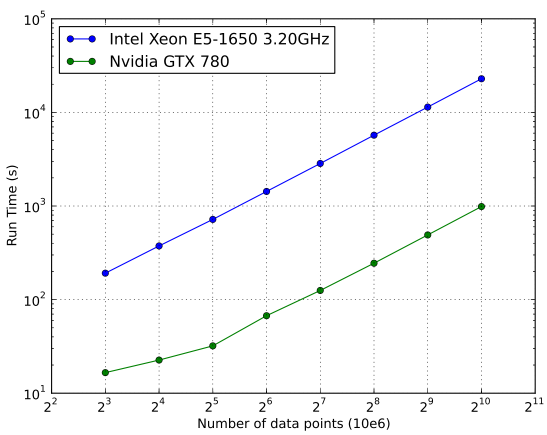

(b) 16 harmonics

Fig. 2.— Run time on makalu machine, with different harmonics.

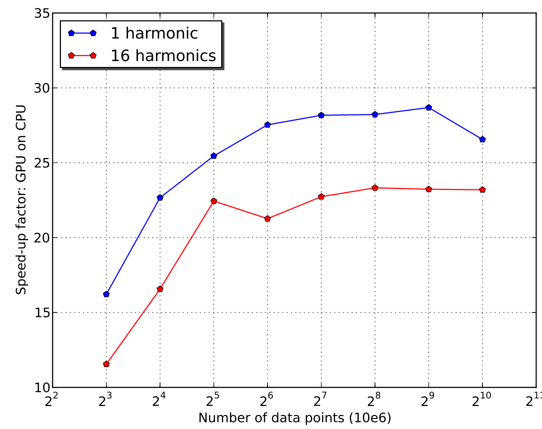

(a) makalu

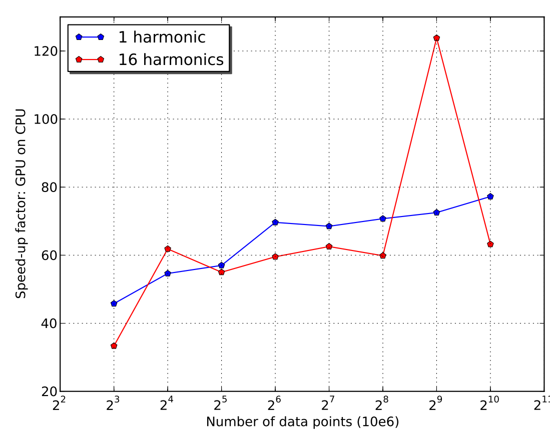

(b) zuul05

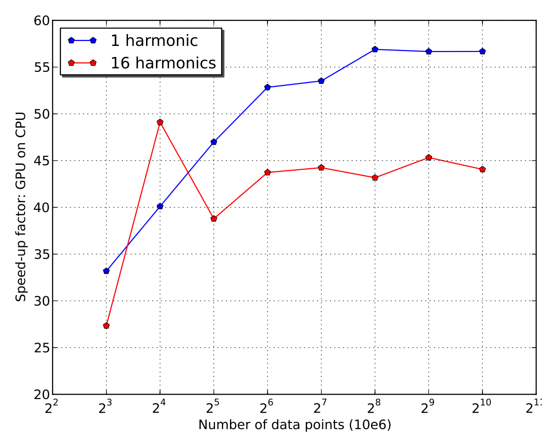

(b) sh machine

Fig. 3.— Speed-up factors: GPU on CPU.

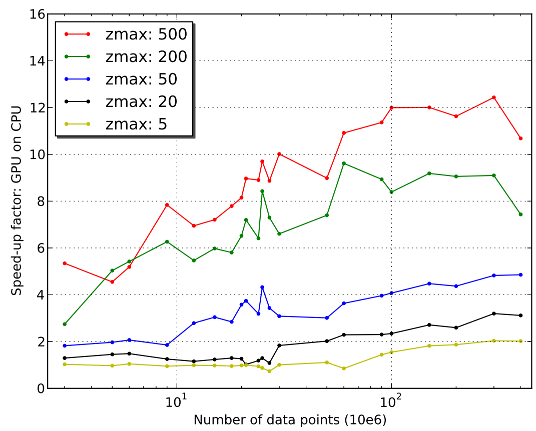

Fig. 4.— Benchmarks on real observation data.

This 2-column preprint was prepared with the AAS LaTeX macros v5.2.